Accepted Manuscript

Research paper

Copper(II) complexes with Box or Flower type Morphology: Sustainability versus Perishability upon catalytic recycling

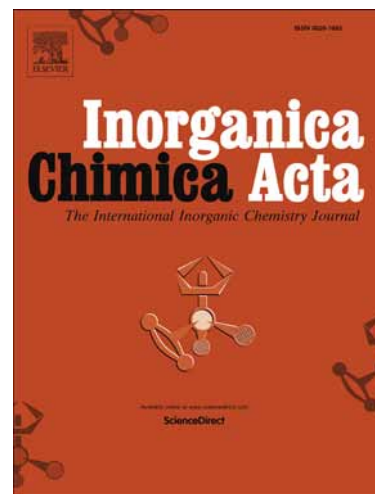Ravinder Kumar, Anjana Yadav, Kuldeep Mahiya, Pavan Mathur

Please cite this article as: R. Kumar, A. Yadav, K. Mahiya, P. Mathur, Copper(II) complexes with Box or Flower type Morphology: Sustainability versus Perishability upon catalytic recycling, *Inorganica Chimica Acta* (2016), doi: http://dx.doi.org/10.1016/j.ica.2016.06.012

Copper(II) complexes with Box or Flower type Morphology: Sustainability versus Perishability upon catalytic recycling

Ravinder Kumar, Anjana Yadav, Kuldeep Mahiya and Pavan Mathur*

Department of Chemistry, University of Delhi, Delhi-110007, India.

Abstract

Copper(II) complexes derived from a benzimidazolyl schiff base ligand are used heterogeneously for the selective oxidation of p-chlorobenzyl alcohol to p-chlorobenzaldehyde. Complex (**1**) shows rectangular box type morphology while complex (**2**) shows a flower like morphology with micropetals. Powder X-ray diffraction pattern upon reuse of catalyst (**1**) shows loss of peaks associated with planes 001 and 100 suggesting preferential exposure of these planes during the catalytic cycle, while the catalyst (**2**) shows loss in activity with planes associated with 011 and 021 (axis b & c) implying a non-preferential activity. It is interesting to note that the box type morphology (**1**) sustains catalysis upon recycling to a greater extent in comparison to the flower type (**2**).

Corresponding Author

Tel: +91 1127667725X1381; Fax: +91 1127666605
***E-mail: pavanmat@yahoo.co.in (P. Mathur)**

1. Introduction

Heterogeneous catalysis provides an opportunity to understand the effect of surface shape/size on the reactivity of the catalyst [1, 2]. Surface chemistry studies have shown that the catalytic selectivity is mainly dependent on the coordination of the substrate on surface [3] and has been found to be affected by the exposed crystallographic facets [4, 5]. Morphology of the catalyst determines the crystal planes that could affect catalysis [6, 7]. The type of morphology like rod, sphere, flower, cuboid and rectangle are known to affect the catalytic reactions since they expose different active planes [8-13]. Few studies have been reported wherein changes in size distribution of the catalyst after recycling have been reported along with catalytic activity [14-15]. Several studies are reported that utilise Cu(II) or Cu(I) halides or insitu generated phenanthroline copper complexes for the oxidation of benzylic alcohols to aldehydes. Some of these reports carry out reactions under refluxing condition under molecular oxygen and in solvent media like H_2O, benzene, DMF-benzene with yields between 55-95%.[16, 17,18-21].

In the present study we have synthesized two new monomeric copper(II) complexes with a benzimidazolyl schiff base ligand. The single crystal X-ray diffraction (SCXRD) reveals that copper(II) complex forms a distorted square planer geometry. Both the complexes are employed for the oxidation of p-chlorobenzyl alcohol to the corresponding aldehyde in dichloromethane using TBHP as oxidant monitored by UV spectral study. The complexes are insoluble in dichloromethane and act as catalyst under heterogeneous conditions at room temperature. The reaction conditions employed are much milder in the present case, and room temperature reaction is carried out with product yields that are comparable to some of the earlier reports. The catalyst is recovered and recycled; the changes that occur in the morphology of the catalyst during reaction are analyzed through scanning electron microscopy (SEM), Powder-XRD, X-ray photon spectroscopy (XPS).

2. Experimental

2.1. Materials and Methods

All chemicals o-Phenylenediamine (Thomas Baker, Mumbai), β-Alanine(Merck), 2-Hydroxy-1-Naphaldehyde (Alfa-Aesar), K_2CO_3(Thomas Baker), $CuCl_2.5H_20$ (Thomas Baker), KCNS, alcohol(Merck) and 70% Tert.butyl hydroperoxide (Lancaster) were used as obtained. 2-aminoethylbenzimidazole dihydrochloride (AB.2HCl) was prepared according to the procedure as reported by Cescon and Day [22].

2.2. Physical Measurements

Elemental analysis of the ligand and their complexes were obtained on VARIO EL III from USIC, University of Delhi, India. IR spectra were recorded on a Perkin-Elmer FT-IR-2000 spectrometer using KBr discs in the range of 400-4000 cm^{-1}. UV-Vis spectra were recorded in DMF with a Shimadzu UV-Vis-1601 spectrometer. Cyclic Voltammetry studies were performed on BAS CV 50W instrument. The cyclic voltammograms were obtained in DMSO: CH_3CN containing 0.1 M Tetrabutyl ammoniumperchlorate (TBAP) as a supporting electrolyte. A three-electrode configuration composed of a Pt disk working electrode, a Pt wire counter electrode, and an $Ag/AgNO_3$ reference electrode was used for the measurements. The morphological changes in the copper(II) complexes was studied by scanning electron microscopy (SEM) model FEI Quanta 200F with oxford –EDS system IE 250 X Max 80 with gold coating in SMITA research lab IIT Delhi, India. GC-MS spectra were recorded at AIRF, JNU, New Delhi on a GCMS-QP2010 (plus) Schimadzu instrument. The powder X-ray diffraction patterns were recorded using High resolution D8 Discover Bruker diffractometer, equipped with point detector (scintillation counter), employing monochromatized Cu K$_{\alpha1}$ radiation with a scan rate of 1.0 second/step and step size 0.02° at 298 K over the range of 2θ = 5°-35°.

3. Synthesis and analysis

3.1. Synthesis of Ligand and its Copper(II) complexes

[C$_{20}$H$_{17}$N$_3$O] (L)

The Schiff base was synthesized as reported earlier [14a]. 2-aminoethyl benzimidazolyl dihydrochloride (AB.2HCl) was neutralized by adding requisite amount of aqueous K_2CO_3. A stirred methanolic solution of 2-hydroxy-1-naphthaldehyde was added slowly to the above solution. After about ½ h a yellow solid separated out. The solid was dried over P_2O_5 and finally recrystallized from acetonitrile. Melting Point 213°C, m/z 316 (M+1).

3.2. Synthesis of Copper(II) complexes

[Cu(L)Cl].MeOH (1)

To a stirred solution of **L** (78 mg, 0.25 mmol) in 15 ml methanol CuCl$_2$.2H$_2$O (43 mg 0.25 mmol) dissolved in 5 ml methanol was added drop wise with constant stirring and the resulting reaction mixture was refluxed for 2 hr at room temperature. Thereafter the reaction mixture was

3

concentrated to one half of its volume on a water bath and allowed to stand at room temperature. A green colored product formed was washed with cold methanol, filtered, air dried. The compound analyzes for the composition $C_{20}H_{16}ClCuN_3O$. MeOH, Yield: 76%; m.p.: 215°C. Single crystal suitable for XRD work were obtained by redissolving the compound in 25-30 ml of hot MeOH and allowed to stand at room temperature. After a few days green colored crystals separated out. Anal. Found(Calc.) for $C_{21}H_{20}N_3O_2CuCl$: C 56.57(56.63), H 4.75(4.53), N 9.48(9.43); Selected IR(KBr, cm^{-1}) $\nu_{(-C=N-C=C-)}$ 1429, $\nu_{(NH)(H\text{-bonded})}$ 3125, $\nu_{(C=N)}$ 1603, $\nu_{C=C}$ benzene 748; UV-Vis λ_{max}/nm (log ε) in DMF: 271(4.3), 283(4.1), 314(4.0), 394(3.8), 634(2.3).

[Cu(L)SCN] (2)

To a methanolic solution (10 ml) of $CuCl_2.2H_2O$ (43 mg, 0.25 mmol), KCNS (25 mg, 0.25 mmol) dissolved in 5 ml methanol was added drop wise until KCl precipitated out. The resulting brown colored solution of $Cu(SCN)_2$ solution was treated with the ligand **L1** solution in methanol. The resulting mixture was warmed at ~80°C for 3 hrs. Thereafter the brown coloured solution so obtained was filtered and transferred to a 100 mL beaker. The solution was allowed to stand at room temperature for few days. Brownish green coloured crystals were collected, and air dried. They analyzed for the composition $C_{21}H_{16}CuN_4OS$. Yield: 72%. m.p.: 187°C

Anal. Found(Calc.) C 57.28(57.85), H 3.58(3.70), N 12.39(12.85), S 8.10(7.35); Selected IR(KBr, cm^{-1}); $\nu_{(-C=N-C=C-)}$ 1457, $\nu_{(NH)(H\text{-bonded})}$ 3190, $\nu_{(C=N)}$ 1603, $\nu_{C=C}$ benzene 738; UV-Vis λ_{max}/nm(log ε) in DMF: 270(3.8), 278(3.7), 313(3.5), 391(3.53, 682(1.8).

3.3. X-ray crystallography

Single crystals of complexes **(1)** and **(2)** suitable for X-ray diffraction studies were grown by slow evaporation in methanol**.** The intensity data for **(1)** were collected at 150(2) K on a Bruker SMART Apex CCD diffractrometer using graphite monochromator (Mo-K$_\alpha$ radiation, λ = 0.71073 Å) from IIT Roorkee India. The intensity data for **(2)** was collected at 298(2) K on an X'calibur CCD diffractometer with graphite monochromatized Mo/Kα. Radiation (λ=0.71073 Å) from USIC, University of Delhi, Delhi, India. For **(1)**, a total of 10759 reflections were measured of which 3060 were unique and 2506 were considered observed ($I > 2\sigma$ (I)]. For **(2)**, a total of 12364 reflections were measured of which 3191 were unique and 2821 were considered observed ($I > 2\sigma$ (I)]. The data were corrected for Lorentz and polarization effects. Multi-scan absorption correction was applied. The structure was solved by direct methods using SHELXS-

4

97^{17} and refined by full-matrix least-squares refinement techniques on F^2, using SHELXL-97 [23]. All calculations were done with the help of WINGX programme [24] For the molecular graphics, the programme Diamond2 [25] and Mercury [26] were used. All non-hydrogen atoms were refined anisotropically. All hydrogen atoms were fixed geometrically with U_{iso} values of 1.2 times the U_{iso} values of their respective carrier atoms. The final residual index for (**1**) are; R 0.0367, Rw 0.0820 for the observed and R 0.0869, Rw 0.0976 for all reflections using 257 parameters and one restraint. The final residual index for (**2**) are; R 0.0801, Rw 0.1891 for the observed and R 0.0886, Rw 0.1943 for all reflections using 253 parameters and zero restraints. Details of the crystallographic data and structure refinement for complexes (**1**), and (**2**) are given in Table 1.

4. Results and Discussion

4.1. Molecular Structure Description of [Cu(L)Cl]. MeOH (1) and [Cu(L)NCS] (2)

The crystal structure of copper(II) complexes (**1**) and (**2**) shows that the ligand coordinates in a tridentate mode with imine nitrogen of the benzimidazole ring, deprotonated napthanol oxygen and the azomethine nitrogen of the ligand. Anionic chloride or thiocyanate also binds to copper to complete the distorted square plane (Figure 1, Table S1) [27, 28]. It is found that the sum of the bond angles about Cu(II) are 375° and 369° for the Cl bound and the NCS bound complexes, suggesting that the Cu(II) atom sits slightly out of square plane. Moreover The the Cu—Cl bond is much longer than the remaining three bond lengths of the square plane contributing to the distortion of the geometry about Cu(II). Selected bond length and angles are given in Table S2.

The hydrogen atom that is attached to the oxygen of methanol present outside the crystal lattice shows H-bonding with the Cl. The extended self-assembled 2D framework is formed by H-bonding interaction (Figure S1). Similarly the hydrogen atom attached to benzimidazole nitrogen shows intermolecular H-bonding with the sulphur of the NCS group forming an extended self-assembled framework in complex (**2**) (Figure S2). The π-π stacking interactions are present in the crystal packing of complex (1) and (2). The crystal packing of (1) and (2) viewed from the *b* axis is shown in Figure S3. In complex (1) benzimidazole ring in one layer is stacked over benzimidazole ring of neighboring molecule (distance between the centroids 3.744 Å) while naphthol ring is stacked over naphthol ring of the neighboring molecule (distance between the

centroids 3.777 Å). Other layers show the same pattern. The interaction between the two layers is weak because the distance between the centroid of benzimidazole and naphthol ring is 4.619 Å. On the other hand complex (2) forms a *zig-zag* structure. Unlike complex (1), the benzimidazole ring stacks over the naphthol ring while the naphthol ring stacks over the benzimidazole ring of the neighboring molecule. The subsequent layers are almost equidistant from each other (distance between the centroids is 3.908 and 4.094 Å). The zig-zag pattern of stacking may have some implications in the generation of petals in flower type morphology.

4.2. Characterizations

4.2.1. Electronic spectroscopy

The UV spectra of the ligand and complexes show absorption maxima in the range of 270-420 nm in DMF, assigned to intraligand **π-π*** transition of the benzimidazole moiety. The **n-π*** transition is assigned to the azomethine (–N=CH-) and a LMCT from the napthanol oxygen to an empty d-orbital of metal ion [29]. A broad but a much less intense d-d band due to copper(II) is observed at 634 nm for complex **(1)** and 682 nm for complex **(2).**

4.2.2. Cyclic Voltammetry

Cyclic voltammograms of both the complex were recorded in mixed CH_3CN: DMSO (3: 2) solution at room temperature with tetrabutylammonium perchlorate (TBAP) as supporting electrolyte. Both the complex shows quasi-reversible peak for the couple Cu(II) ↔ Cu(I) (Figure S5 and Figure S6). The $E_{1/2}$ values are found to be -36.5 mV for complex **(1)** and +49.6 mV for complex **(2)** respectively.

5. Catalytic Activity study

[Cu(**L**)Cl].MeOH **(1)** and [Cu(**L**)NCS] **(2)** were used heterogeneously for the oxidation of p-chloro benzyl alcohol to its respective aldehyde and monitored by UV-spectroscopy Figure 2. In a typical reaction, benzyl alcohol, catalyst, oxidant in a ratio of 5: 1: 7 respectively were mixed in 15 mL dichloromethane and stirred at 35-40° C on a water bath for a 4 hrs.the reaction mixture was centrifuged after a 4 hr reaction to isolate the copper(II) catalyst, for further reuse. The clear filterate of the reaction mixture was checked for any dissolution of the catalyst during reaction, no d-d band in the visible range of 500-900 nm was observed,suggesting no/minimal dissolution

of the copper(II) catalyst. The complexes were reused for the oxidation reaction and a decrease in the yield of benzaldehyde was observed, as analyzed through GC-MS. Both the complexes are reused three times and their percentage conversions for the repeat cycle are summarized in Table 1. The oxidation of p-chlorobenzyl alcohol was monitored spectrophotometrically by measuring the increase in the characteristic p-chlorobenzaldehyde absorption band at 256 nm as a function of time [15a].

6. SEM and PXRD Analysis

In order to observe the impact of surface morphology on catalysis during recycling, the catalyst was recovered after the oxidation reaction was complete. A gold coated sample of the recovered catalyst was prepared for SEM measurement. The SEM micrograph shows that the mononuclear complex (**1**) before use as catalyst has a rectangular box like morphology where the average length of boxes lies between 75-140 μm for complex (**1**) (Figure 3**A**). Its subsequent reuse in the catalytic oxidation of *p*-chlorobenzyl alcohol causes the morphology to change to a more or less flat 2-dimensinal boxes (wafer type) with length varying from 25-40 μm for complex (**1**) (Figure 3**B**).

The thiocyante bound mononuclear complex (**2**) is found to possess a flower like morphology [30] and contains petals. The micro-petals are flat and the length of each petal ranges from 1.3 to 1.01 μm (Figure 3**C**). After 3rd use the petals shows a shortening in length upto 0.86 μm, while some petals are found to conjoin together, giving rise to cluster formation (Figure 3**D**). The morphology changes for the thiocyante bound monomeric complex are more apparent upon reuse in comparison to the chloride bound complex, and may explain the sharp drop in percentage conversion of alcohol to aldehyde that varies from 74% to 48% for complex (**2**)**.** In comparison the complex (**1**) upon reuse shows a change from 68% to 52% for the formation of aldehyde.

The powder XRD pattern of both the complexes also shows changes that occur after successive use of the catalyst for the oxidation of p-chlorobenzyl alcohol to p-chlorobenzaldehyde. The monomeric copper (II) complex (**1**) shows that the parent complex has sharp intense peaks at 2θ (hkl) 7.6(001), 8.8(010), 11.5(100), 12.7(110), 14.3(101) 17.8(002), 21.8(020) and 26.8(202). After reuse major changes occur in the low intensity at peaks 7.6(001) and 11.5(100), each plane exposing a single axis (a or c). The thiocyante bound complex (**2**) also shows sharp peak at 2θ 10.1(011), 11.3(021), 16.2, 24.4, 25.8(080), 29.2 and 30.6. After reuse major changes occur in

7

the low intensity of peaks at 10.1(011) and 11.3(021), both planes exposing two axis (b & c). This suggests that the diffraction planes undergoing changes could be involved in the promotion of catalysis for complex **(1)** and **(2)** (Figure 4).

6.1. d-d band Variation

The d-d band spectral changes were measured by making a 3.8 mmolar solution of the used complex (1) and measuring its visible spectra (Figure. S7). It is interesting to note that after repeat cycles there is drop in the d-d band intensity in visible region. The complex shows a drop in d-d band intensity by 22% upon reuse for complex **(1)** (Figure S7). A similar loss in d-d band intensity is also observed for complex (2). The loss in d-d band intensity is an indication of the formation of copper (I) during catalytic cycle and could be related to loss in catalytic activity. Formation of Cu(I) species has been observed earlier also [31].

6.2. X-Ray Photoelectron Spectroscopy

The [Cu(L)NCS] complex shows two main peaks at 935eV and 955eV with a satellite peak at 945eV. These peak positions have been reported to be associated with copper in +2 oxidation state [32] (Figure 5). The XPS of the reused complex shows the presence of a new shoulder, observed at 933eV (Figure 5 inset) along with peaks at 935eV, 953eV with a satellite peak at 942eV [33]. The appearance of a prominent shoulder at 933eV has been reported to be due to copper in +1 oxidation state [33]. This shows that the reused complex has some proportion of copper(I) species besides copper(II) complex.

7. Conclusion

Catalyst (**1**) shows bigger rectangular boxes (120-150 μm) which change to smaller boxes (30-50 μm) as indicated by SEM after catalysis. Some planes diminish in intensity as observed by PXRD and could be responsible for the inactivation of the catalyst. Smaller drop in percentage conversion ≈16% upon reuse, suggesting relatively sustained catalysis upon reuse.

Catalyst (**2**) shows flower type morphology where the petal size change from 1.01 to 0.86 μm upon reuse. The interaction of the catalyst with the substrate results in clustering of the petals that possibly blocks the catalytic cycle step. Sharp change in percentage conversion from 74% to

8

48% upon reuse implying that there is an initial higher catalytic activity with flower type morphology but it perishes quickly and does not sustain a higher velocity of activity upon reuse.

Since the complexes are insoluble in the medium of reaction (dichloromethane) and dissolution of copper(II) catalyst is minimal, hence the major catalytic reaction proceeds via a heterogeneous rather than homogeneous pathway. A tentative reaction scheme is depicted in Scheme I.
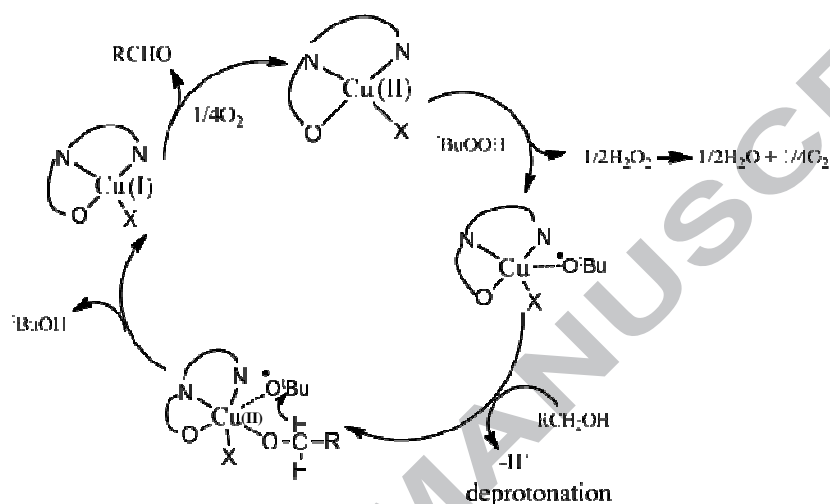
Scheme I

Acknowledgment

Supplementary Material

CCDC 883788 and 883786 contain the supplementary crystallorgaphic data for this paper. These data can be obtained free of charge from The Cambridge Crystallographic Data Centre via www.ccdc.cam.ac.uk/data_request/cif. H-bonding interactions for both the complexes. Crystallorgaphic data and selected bond length and angles.

REFERENCES

1. (a) D. Zhang, X. Du, L. Shi, R. Gao, Dalton Trans., 41 (2012) 14455. (b) G. R. Jenness, J. R. Schmidt, ACS Catal. 3 (2013) 2881.

2. (a) C. Burda, X. B. Chen, R. Narayanan, M. A. El-Sayed, Chem. Rev., 105 (2005) 1025. (b) J. A. van Bokhoven, Chem Cat. Chem., **1** (2009) 363.

3. R. A. Van Santen, M. Neurock, S. G. Shetty, Chem. Rev., 110 (2010) 2005.

4. F. Zaera, Acc. Chem. Res., 42 (2009) 1152.

5. (a) G. A. Somorjai, Chem. Rev., 96 (1996) 1223; (b) C. R. Henry, Surf. Sci. Rep., 31 (1998) 231. (c) L. Vattuone, L. Savio, M. Rocca, Surf. Sci. Rep., 63 (2008) 101.

6. (a) Y. Li, W. Shen, Chem. Soc. Rev. 43 (2014) 1543 (references there in). (b) X. Du, D. Zhang, L. Shi, R. Gao, J. Zhang, J. Phys. Chem. C, 116 (2012) 10009.

7. (a) Y. Li, Q. Liu, W. Shen, Dalton Trans., 40 (2011) 5811. (b) N. V. Long, C. M. Thi, M. Nogami, M. Ohtaki, New, J. Chem., 36 (2012) 1320.

8. R. Narayanan, M. A. El-Sayed, J. Am. Chem. Soc., 126 (2004) 7194.

9. C. I. Carlisle, T. Fujimoto, W. S. Sim, D. A. King, Surf. Sci. 470 (2000) 15.

10. (a) J. M. Hawkins, J. F. Weaver, A. Asthagiri, Phys. Rev. B 79 (2009) 125434. (b) S. P. Devarajan, J. A. Hinojosa, J. F. Weaver, Surf. Sci. 602 (2008) 3116.

11. (a) H. X. Mai, L. D. Sun, Y. W. Zhang, R. Si, W. Feng, H. P. Zhang, H. C. Liu, C. H. Yan, J. Phys. Chem. B, 109 (2005) 24380. (b) R. Narayanan, M. A. El-Sayed, J. Phys. Chem. B, 125 (2003) 8340.

12. (a) K. Zhou, X. Wang, X. Sun, Q. Peng, Y. Li, J. Catal., 229 (2005) 206. (b) S. Kim, S. U. Son, S. S. Lee, T. Hyeon, Y. K. Chung, Chem. Commun., (2001) 2212.

13. (a) N. Ta, M. L. Zhang, J. Li, H. J. Li, Y. Li, W. Shen, Catal. Today, 148 (2009) 179. (b) J. Sculz, A. Roucoux, H. Patin, Eur. J. Chem., 6 (2000) 618. (c) F. Gao, D. W. Goodman, Annu. Rev. Phys. Chem., 63 (2012) 265.

14. (a) R. Kumar, K. Mahiya, P. Mathur, Dalton Trans., 42 (2013) 8553-8557. (b) R. Narayanan, M. A. El-Sayed, J. Phys. Chem. B, 107 (2003) 12416.

15. (a) K. Mahiya, P. Mathur, Inorg. Chim. Act. 399 (2013) 36. (b) N. Tian, Z. Y. Zhou, S. G. Sun, Y. Ding, Z. L. Wang, Science, 316 (2007) 732.

16. Liang, L.; Rao, G.; Sun, H.-L.; Zhang, J.-L. Adv. Synth. Catal. 2010, 352, 2371.

17. Lahtinen, P.; Ahmad, J. U.; Lankinen, E.; Pihko, P.; Leskelä, M.; Repo, T. J. Mol. Catal. A: Chem. 2007, 275, 228.

18. Jallabert, C.; Riviere, H. Tetrahedron Lett. 1977, 18, 1215.

19. Jallabert, C.; Riviere, H. Tetrahedron 1980, 36, 1191.

20. Jallabert, C.; Lapinte, C.; Riviere, H. J. Mol. Catal. 1982, 14, 75.

21. Lahtinen, P.; Korpi, H.; Haavisto, E.; Leskelä, M.; Repo, T. J. Comb. Chem. 2004, 6, 967.

22. L. A. Cescon, and A. R. Day, J. Org. Chem, 27 (1962) 581.

23. Oxford Diffraction CrysAlis Software System, Ver. 1.171.32. (Oxford Diffraction Ltd. Abingdon, UK) 2007.

24. G. M. Sheldrick, Acta Crystallogr, A64 (2008) 112. (b) A. L. Spek, J. Appl. Crstallogr, 36 (2003) 7.

25. G. Bergerhoff, M. Berndt, K. Brandenburg, J. Res. Natl. Inst. Stand. Technol. 101 (1996) 221.

26. C. F. Macrae, P. R. Edgington, P. McCabe, E. Pidcock, G. P. Shields, R. Taylor, M. Towler, J. V. De Streek, J. Appl. Crystallogr. 39 (2006) 453.

27. (a) M. E Bluhm, M. H. Ciesielski, G. O. Walter, M. Doring, Inorg. Chem., 42 (2003) 8878. (b) H. Wang, Y. Lang, S. Wang, Act. Cryst. E68 (2012) m540. (c) P. Talukder, A. Datta, S. Mitra, G. Rosair, M. S. El Fallah, J. Ribas, Dalton Trans. (2004) 4161.

28. C. S. Rajarajeswari, R. Loganathan, M, Palaniandavar, E. Suresh, A. Riyasdeend, M. A., Akbarshae, Dalton Trans. 42 (2013) 8347.

29. R. Kumar. K. Mahiya and P. Mathur. Ind. J. Chem. 50A (2011) 775.

30. (a) P. Kumar, M. Gusain, R. Nagarajan, Inorg. Chem. 50 (2011) 3065. (b) G. Tong, J. Yuan, W. Wu, Q. Hu, H. Qian, L. Li, J. Shen, CrystEngComm. 14 (2012) 2071.

31. S. Tehlan, M. S. Hundal, P. Mathur, Inorg. Chem. 43(21) (2004) 6589.

32. (a) U. G. Singh, R. T. Williamsa, K. R. Hallam, G. C. Allen, J. Solid State Chem. 178 (2005) 3405. (b) H. Ripp, U. Weser, Bioinorg. Chem., 6 (1976) 45.

33. L. N. Mazalov, S. V. Trubina, G. K. Parygina, I. M. Oglezneva, E. A. Aseeva, N. V. Brenner, E. U. Fursova, V. I. Yovcharenko, J. Struct. Chem. 47(3) (2006) 558.
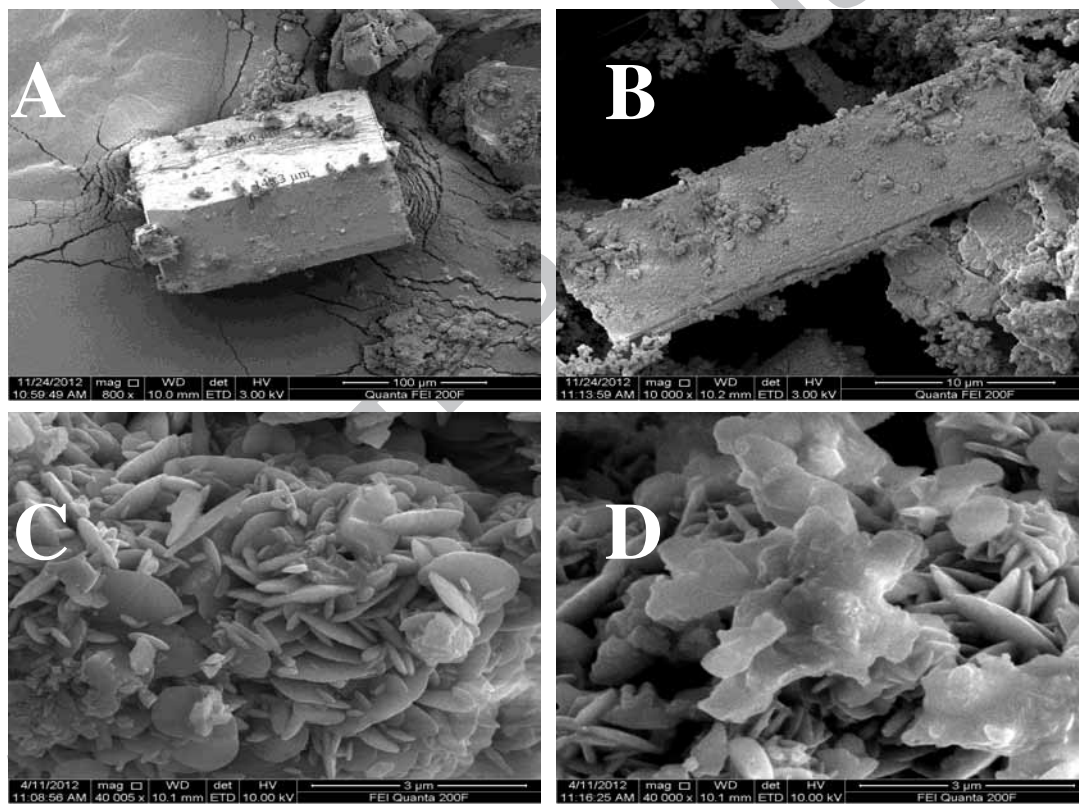
Figures and Table
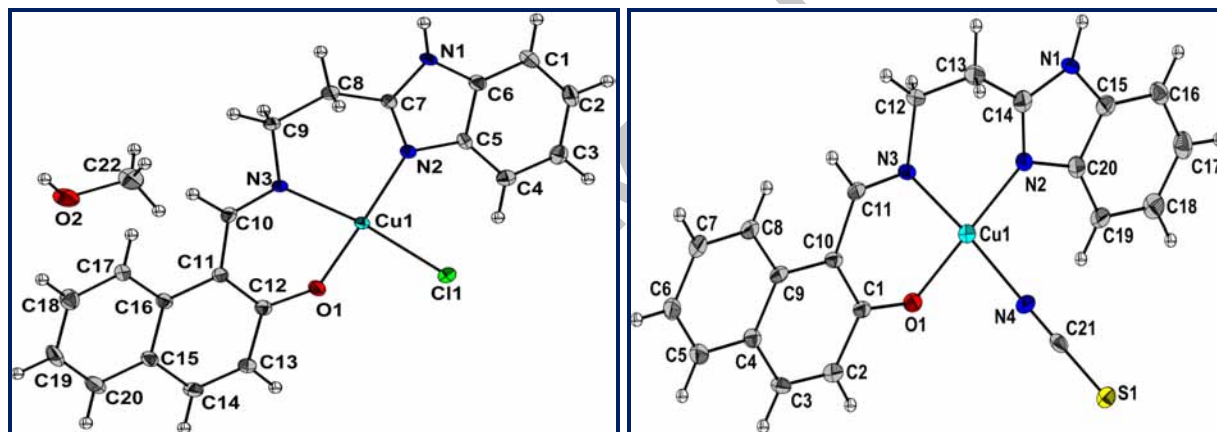
Figure 1. ORTEP diagram of the **[Cu(L)Cl].MeOH (1)** and **[Cu(L)NCS] (2)** drawn in 30% thermal probability ellipsoids with atomic numbering scheme.
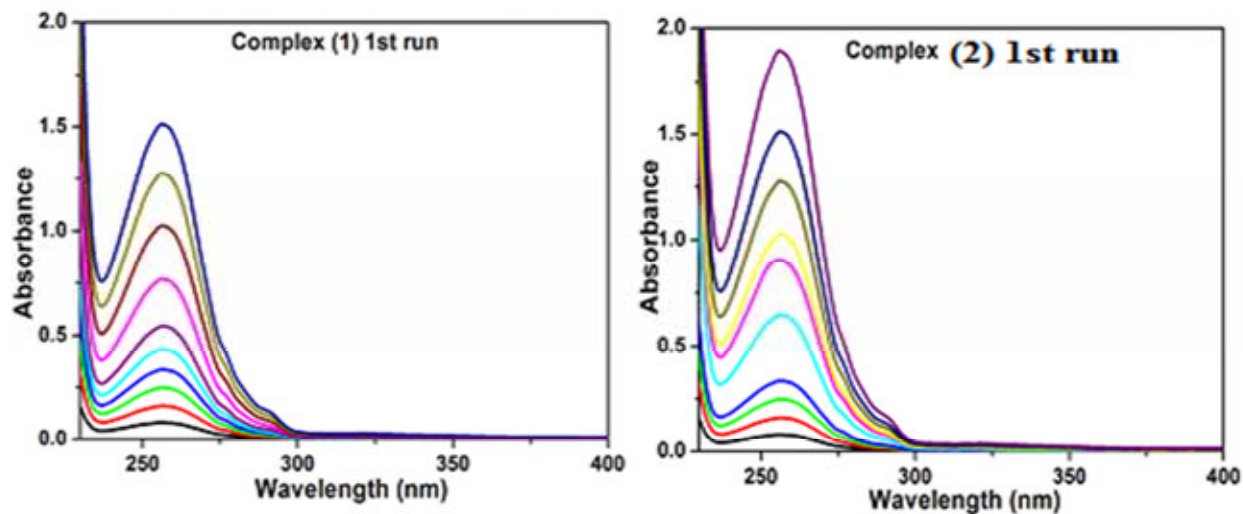
Figure 2. Time dependent UV-Visible absorbance spectra for the formation of p-Cl-Benzaldehyde for every 10 min time interval. Complex (**1**): 1st run (**2**): 1st run.

Figure 3. Variation in the Morphology of complexes (**1**) and (**2**) during catalysis. A and C represents unused complex; B and D represents complex after 3rd use in catalysis.
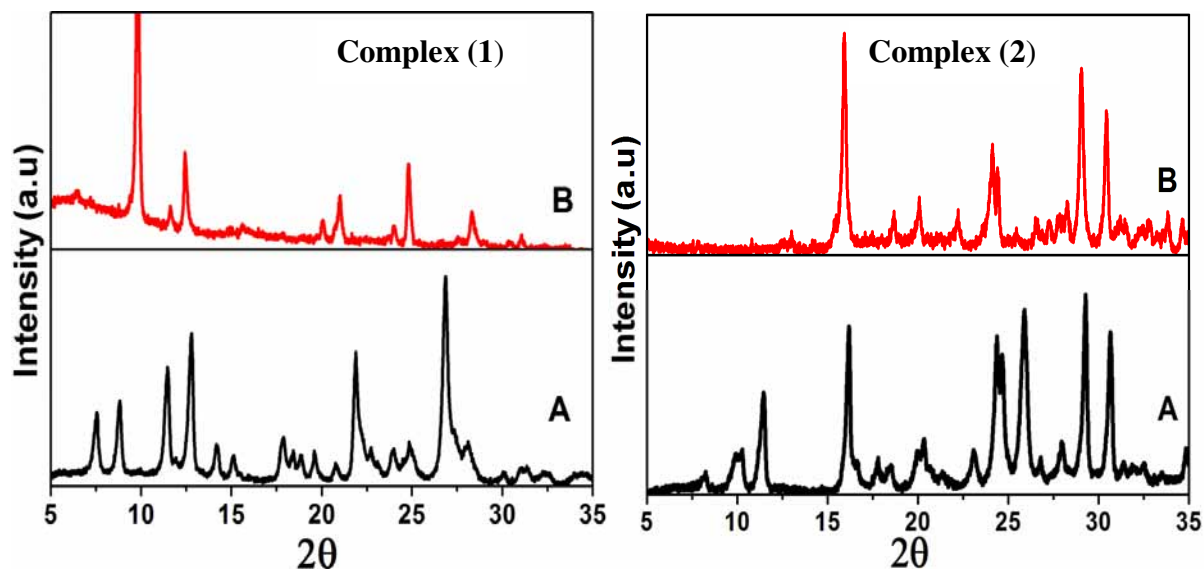
13

Figure 4. PXRD pattern of complexes **(1)** and **(2): (A)** Unused complex **(B)** After 3rd use
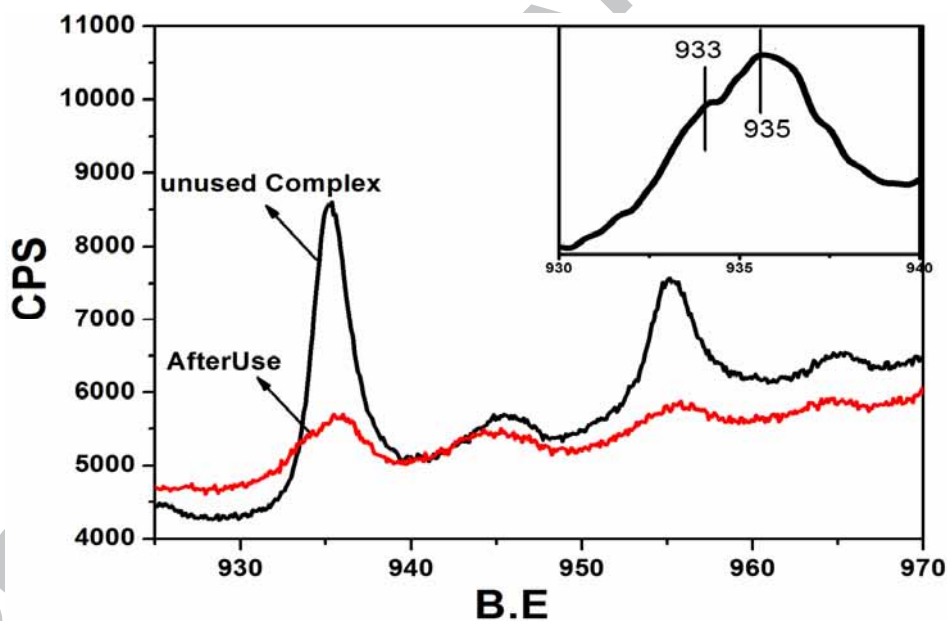

Figure 5. XPS spectra of complex [Cu(**L**)NCS] **(2)** unused complex and after 3[rd]use in catalysis
Inset: Blow up of formation of new peak at 933 eV generated after reuse of the catalyst.

Table

Table 1. % conversion of oxidation reaction of p-chlorobenzyl alcohol to the aldehyde of complexes

Catalyst	Reusability	Yield (%)
[Cu(L)Cl] (1)	1st use	68
	3rd use	52
[Cu(L)NCS] (2)	1st use	74
	3rd use	48

*Based on GC-MS with naphthalene as Internal Standard
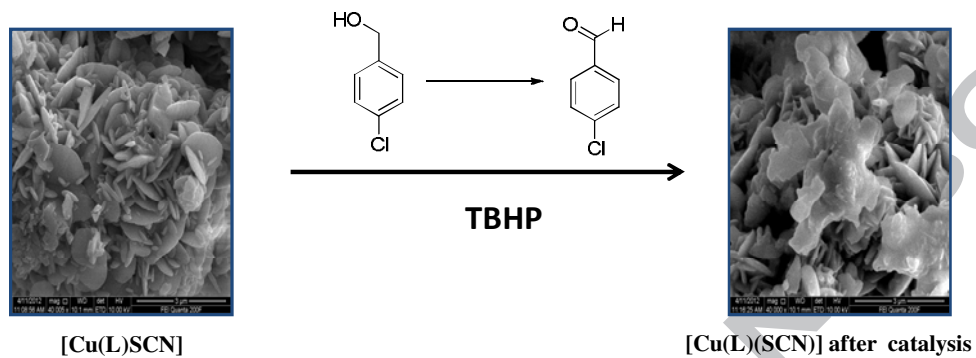
Graphical abstract
Copper(II) complexes with Box or Flower type Morphology: Sustainability versus Perishability upon catalytic recycling

Ravinder Kumar and Pavan Mathur*

Department of Chemistry, University of Delhi, Delhi-110007, India.

TBHP

[Cu(L)SCN]   **[Cu(L)(SCN)] after catalysis**

Synopsis

Selective oxidation of p-chlorobenzyl alcohol to p-chlorobenzaldehyde is carried out by new copper(II) complexes of a benzimidazolyl schiff base ligand. Efficiency of oxidation depends on the morphology of the complexes; box type morphology sustains catalysis upon recycling to a greater extent in comparison to the flower type.

Highlights

1. Monomeric copper(II) complexes of a benzimidazolyl schiff base ligand.

2. Oxidation of p-chlorobenzyl alcohol to p-chlorobenzaldehyde, heterogeneously.

3. Rectangular box type morphology found for [Cu L Cl] while flower type with micro petals for [Cu L SCN].

4. Loss of PXRD peaks associated with certain planes with reuse of catalyst .

5. Box type morphology sustains catalysis upon recycling compared to the flower type.